Journal of Alloys and Compounds 655 (2016) 327–335

Contents lists available at ScienceDirect

Journal of Alloys and Compounds

journal homepage: http://www.elsevier.com/locate/jalcom

Strain dependence of the physical properties of epitaxial $La_{0.7}Ca_{0.3}MnO_3$ thin films grown on $LaAlO_3$ substrates

S. El Helali [a, *], K. Daoudi [b, c], M. Boudard [d], A. Schulman [d, e], C. Acha [e], H. Roussel [d, e], M. Oumezzine [a], M. Oueslati [b]

[a] Laboratoire de Physico-Chimie des Matériaux, Faculté des Science de Monastir, University of Monastir, 5018 Monastir, Tunisia
[b] Unité Nanomatériaux et Photonique, Faculté des Sciences de Tunis, Tunis El Manar University, 2092 El-Manar Tunis, Tunisia
[c] Department of Applied Physics, College of Sciences, University of Sharjah, P.O. Box 27272, Sharjah, United Arab Emirates
[d] LMGP, Univ. Grenoble Alpes, CNRS, Grenoble F-38000, France
[e] Departamento de Física, FCEyN, UBA and IFIBA, Conicet, Pabellón 1, Ciudad Universitaria, 1428 Buenos Aires, Argentina

ARTICLE INFO

Article history:
Received 28 March 2015
Received in revised form
27 August 2015
Accepted 14 September 2015
Available online 15 September 2015

Keywords:
LCMO
Strain
Transport properties
Colossal magnetoresistance

ABSTRACT

We present a systematic study of the structural, magnetic, electrical and magnetoresistive properties of $La_{0.7}Ca_{0.3}MnO_3$ thin films epitaxially grown on $LaAlO_3$ single crystalline substrates using metal organic deposition process. The evolutions of the lattice parameters and the corresponding strain as a function of the film thickness (20–80 nm) have been investigated using X-ray diffraction measurements. The films were found to be totally relaxed for a thickness around 60 nm. Magnetization and resistance measurements as a function of temperature revealed a direct correlation of the transition temperature from a ferromagnetic state to the paramagnetic state with the film thickness. The temperature dependence of the resistivity (ρ (T)) has been fitted using various theoretical approaches. Below the transition temperature (T_P) the ρ (T) graphs were well fitted using the $\rho(T) = \rho_0 + AT^{\alpha}$ formula, in which the fitting parameters ρ_0 and α have been used to clarify the conduction mechanism. Above T_P the ρ (T) graphs were found to be well fitted using different models including the VRH model and the small polaron model. A magnetoresistance of 91% was measured at 248 K for the for 60 nm thick film under an applied magnetic field of 7 T. As well as a non-volatile resistive switching capacity of 15% on Ag contacts deposited on top of this film.

1. Introduction

The perovskite manganite $La_{1-X}A_XMnO_3$ (A = Alkaline earth) have attracted considerable attention because of their unusual magnetic and transport behaviors such as colossal magnetoresistance (CMR) [1,2]. These materials are characterized by a rich and complex phase diagram caused by the competition among spin, charge, orbital and lattice degree of freedom [3,4]. The $La_{1-X}Ca_XMnO_3$ in the doping levels $0.25 < x < 0.33$ shows a CMR characteristics combining simultaneous metal-insulator (MI) and ferromagnetic–paramagnetic (FP) transition [5,6] in temperature $200\ K < T_P < 300\ K$. Also, these materials are known by a large coefficient temperature (TCR) [7]. This makes them key materials for magnetic random access memories, magnetic sensors, and various spintronics devices [8]. Moreover, interfaces made of these materials (as well as other perovskite oxides) with a metal have shown non-volatile and reversible resistance properties, making them suitable to perform resistive random access memories (RRAM) [9,10].

In bulk material, physical properties are correlated to alkaline site which modify the Mn^{3+} to Mn^{4+} and in turn will affect the structure of the coupled system MnO_6 octahedra [11]. Furthermore, in thin film form, these intrinsic physical properties can be affected by the growth method, the deposition parameters and also the substrate-induced strain [12,13].

We recently investigated the transport properties dependence on the substrate material [14]. The LCMO having a thickness of 40 nm have been epitaxially grown on single crystalline $LaAlO_3$ (LAO), $SrTiO_3$ (STO) and $(LaAlO_3)_{0.3}$–$(SrAlTaO_6)_{0.7}$ (LSAT) substrates imposing various strain states. The conduction mechanism is found to be strongly dependent on the lattice mismatch between the film and the used substrate.

* Corresponding author.
E-mail address: saoussen_elhelali@yahoo.fr (S. El Helali).

http://dx.doi.org/10.1016/j.jallcom.2015.09.121
0925-8388/

In this paper we extended our investigation on the effect of the film thickness on the structural, magnetic and electrical transport properties of the LCMO films grown on LAO substrates. The strain is systematically varied by increasing the film thickness from 20 to 80 nm. The structural parameters of the LCMO films have been extracted from the XRD measurements and used to quantitatively determine the evolution of the strain as a function of the film thickness. We present also the correlations between the structural properties and the corresponding, magnetic, electrical transport and magneto-resistance as a function of the induced strain in the films. Additionally, we show the capacity of our films to act as a RRAM memory device based on the resistive switching mechanism.

2. Experimental details

LCMO films were deposited on LAO (001) single crystal substrate using the metal organic deposition (MOD) process [15]. The starting solution was prepared by a mixing constituent metal-naphthenate solution (Nihon Kagaku Sangyo) and diluting with toluene to obtain the required concentration and viscosity. The molar ratios of La, Ca and Mn in the coating solution were 0.7, 0.3 and 1.0, respectively. This solution was spin-coated onto LAO (001) substrate at 4000 rpm for 10 s. To eliminate the toluene, the metal-organic (MO) film was then dried in air at 100 °C for 10 min. Before the final annealing, a preheating step at 500 °C for 30 min is necessary to decompose the organic part. This preheating step is also required to prevent the formation of fissures on the film surface during the final annealing at a high temperature. To obtain a satisfactory film thickness, the above procedure (coating, drying, and preheating) was repeated several times giving rise to a corresponding number of superimposed layers in the LCMO product film. The final annealing was carried out in a conventional furnace at 900 °C for 60 min in air.

Phase purity and film crystallinity were examined by X-ray diffraction (XRD) in Bragg–Brentano geometry using a BRUKER D8 advance diffractometer with monochromatic $CuK_{\alpha 1}$ radiation ($\lambda = 0.154060$ nm) and LynxEye 1 dimension detector. Reciprocal space mappings (RSM) were collected with a RIGAKU Smartlab equipped with a Cu rotating anode (9 kW). An incident high resolution setting was used (1D parabolic mirror and a two-crystal Ge monochromator in the 400 setting) leading to a monochromatic parallel x-ray beam ($CuK\alpha_1$). Optics used after the sample, were two 1.0 mm cross 10.0 mm slits, 2.5° sollers slits and a punctual scintillation counter detector.

Electrical transport measurements were performed using a four-probe technique. Magnetic characterization was performed using a commercial SQUID magnetometer (Quantum Design, 5T) with an applied magnetic field of 500 Oe in both the field cooled (FC) and zero field cooled (ZFC) measurements in the 5–300 K temperature range. We also performed resistive switching hysteresis loop measurements (RSHL), which is a way to test the capacity of a device to act as a memory device. This protocol is useful to characterize the response of the remnant resistance of a device to the amplitude of the applied pulses. The resistance of the LCMO/Ag interface is measured (read operation) after applying current pulses (write operation) of 10 ms following a loop sequence: Iini → Imax → Imin → Iini.

3. Results and discussion

3.1. Structural properties

Fig. 1 shows the θ–2θ XRD patterns around the *002* Bragg reflections of the LCMO films, with different thicknesses ranging from

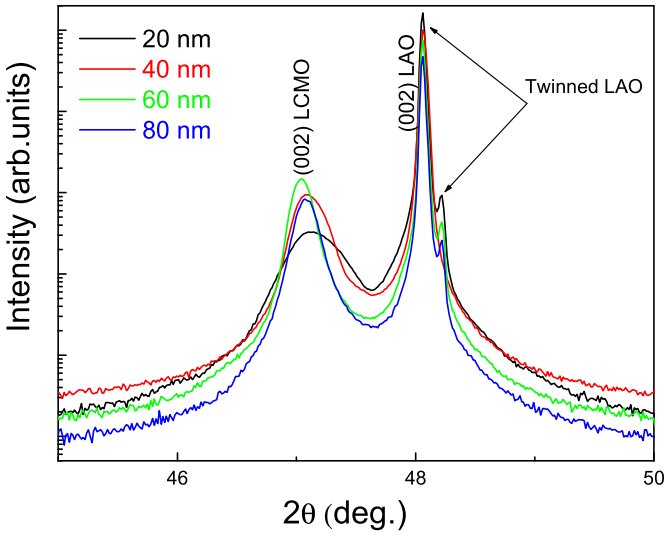

Fig. 1. θ–2θ XRD scans of the LCMO films grown on LAO substrates for different thicknesses.

20 to 80 nm (measured using transmission electron microscopy observations on cross-sections in our previous studies [15]). The LCMO crystallizes into an orthorhombic structure with Pnma symmetry. It is often represented by a pseudo-cubic lattice parameter of 3.858 Å. The lattice parameter of the LAO in the cubic structure is 3.789 Å imposing therefore, an in-plane compressive strain and an out-of-plane compressive strain of 1.84%. The LCMO films grow epitaxially on top of the LAO substrate with common (*00l*) planes orientations (parallels to the surface) i.e. with $[001]_{LCMO}//[001]_{LAO}$ orientation relationship. The splitting of the *002* Bragg peaks of the LAO is due to twinning. By increasing the film thickness from 20 to 80 nm we notice in Fig. 1 some obvious changes in the intensity, the position and the width of the *002* peaks of the LCMO film. The increase in the peak intensity is expected since we increased the quantity of the diffracting material by increasing the film thickness. The *002* LCMO peak is shifted toward lower angles and this correspond to an increase in the out-of-plane parameter "*c*". The out-of-plane lattice parameters have been determined from the θ–2θ XRD scans. Using the "c" parameter, we can extracted the out-of-plane epitaxial strain which can be calculated by the following relation: $\varepsilon_{zz} = (c - c_b)/c_b$, where $\boldsymbol{c}$ is the out-of-plane lattice parameter of the film and $\boldsymbol{c_b}$ is the bulk pseudo-cubic lattice parameter of LCMO. These parameters are listed in Table 1.

The 20 nm thick film has an out-of-plane lattice parameter slightly superior to that one of the bulk LCMO. This small value of the lattice parameter is probably due to the large strain, the poor film crystallinity and the oxygen stoichiometry. By increasing the film thickness for 20 to 40 then 60 nm, the lattice parameter is relatively increased. On reaching the 80 nm thick film, the lattice parameter decreases from 3.863 to 3.860 Å. Considering the cell parameter for bulk LCMO $c_b = 3.858$ Å, the obtained values for *c* indicate that the LCMO is under compressive strain. Furthermore,

Table 1
Out-of-plane lattice parameter (*c*) and the corresponding epitaxial strain (ε_{zz}) of the LCMO films grown on LAO substrates for different thicknesses.

LCMO/LAO	20 nm	40 nm	60 nm	80 nm
c (Å)	3.859 ± 10^{-4}	3.861 ± 10^{-4}	3.863 ± 10^{-4}	3.860 ± 10^{-4}
ε_{zz} (%)	0.026	0.078	0.129	0.052